

absence of interactions. Note that $\epsilon_0 = (\epsilon_0 V)^{-1}$, where V is the volume of the system and ϵ_0 is the average level spacing (per spin) at the Fermi energy. It turns out that both diagrams in Fig. 1 are dominated by momentum transfers of the order of the Fermi momentum k_F , which for a metallic system is large compared with ϵ^{-1} . Eqs. (2) and (3) are therefore not suitable for a quantitatively accurate calculation of persistent currents. To make some progress analytically, AE estimated the contribution from the diagrams in Fig. 1 by replacing the effective interaction by a constant

$$\overline{V}_{\text{RPA}}(\mathbf{k} = \mathbf{k}_F^0; i!) = \overline{V}_{\text{RPA}}(\mathbf{k}_F = \mathbf{k}_F^0; i!) \overline{V}; \quad (4)$$

where \overline{V} denotes the Fermi surface average over k_F and k_F^0 . For simplicity, it is assumed that the ring is quasi one-dimensional, with transverse thickness L_\perp in the range $k_F^{-1} \ll L_\perp \ll L$, where L is the circumference of the ring. Then diffusive motion is only possible along the circumference. At temperature $T = 0$ the resulting average persistent current can be written as⁶

$$\overline{I}^{\text{AE}}(\omega) = \sum_{\mathbf{k} = 1}^{\mathbf{k}_F^0} I_{\mathbf{k}}^{\text{AE}} \sin(4\mathbf{k} \cdot \mathbf{r} = 0); \quad (5)$$

where $\epsilon_0 = \hbar c / e$ is the flux quantum⁷ and the Fourier coefficients of the current are

$$I_{\mathbf{k}}^{\text{AE}} = \frac{c}{\epsilon_0} \frac{16}{k^2} E_c e^{k^2 \epsilon_0} [1 + k^2 \epsilon_0]; \quad (6)$$

Here $E_c = \hbar D_0 / L^2$ is the Thouless energy and $\epsilon_0 = \epsilon_0 / E_c \ll 1$, where at zero temperature $\epsilon_0 = \epsilon_0$ is the cut-off energy that regularizes the singularity in the Cooperon in a finite system⁸, see Eqs. (14) and (20) below. The coupling constant $c = \epsilon_0 V$ can be identified with the dimensionless effective interaction in the Cooper channel to first order in perturbation theory. AE estimated $c \approx 0.3$, assuming that the validity of the RPA can be extended to momentum transfers of the order of k_F . However, higher order ladder diagrams in the Cooper channel strongly reduce the effective interaction, so that $c \approx 0.06$ is a more realistic estimate⁹ for the Cu-rings in the experiment¹.

In real space Eq. (4) amounts to replacing the electron-electron interaction by a local effective density-density interaction,

$$\overline{V}_e(\mathbf{r} = \mathbf{r}') = \overline{V}(\mathbf{r} = \mathbf{r}'); \quad (7)$$

More precisely, this replacement means that for distances $|\mathbf{r} - \mathbf{r}'|$ larger than ϵ^{-1} , the interaction is effectively local. In a recent letter Schechter, Oreg, Imry, and Levinson¹⁰ pointed out that a different type of effective interaction can possibly lead to a much larger persistent current. Specifically, they used the BCS model to calculate the leading interaction correction to the orbital linear magnetic response and found^{7,10}

$$\frac{\partial \overline{I}^{\text{BCS}}}{\partial \epsilon} = \frac{c}{\epsilon_0} 32 E_{\text{BCS}} E_c \ln \frac{E_{\infty}}{\epsilon_0}; \quad (8)$$

where $E_{\text{BCS}} < 0$ is the attractive dimensionless interaction in the BCS model, and the coherence energy E_{∞} is the smaller energy of ϵ_0 and the Debye energy ϵ_D . Eq. (8) should be compared with the corresponding result for the local interaction model used by AE, which implies according to Eqs. (5) and (6),

$$\frac{\partial \overline{I}^{\text{AE}}}{\partial \epsilon} = \frac{c}{\epsilon_0} 32 E_c \ln \frac{E_c}{\epsilon_0}; \quad (9)$$

where we have used $\epsilon_0 = \epsilon_0$ and retained only the leading logarithmic order. Note that the logarithm is due to the slow decay ($\propto k^{-1}$) of the Fourier coefficients $I_{\mathbf{k}}^{\text{AE}} = \epsilon_0$ of $\overline{I}^{\text{AE}} = \epsilon_0$, so that all coefficients with $k \ll 1/\epsilon_0$ contribute to the linear response. For $E_{\infty} \gg E_c$ the linear magnetic response in the BCS model is parametrically larger than the linear response in the local interaction model. Whether or not this remains true beyond the linear response has not been clarified. Note also that in the BCS model the linear magnetic response is diamagnetic because the effective interaction is attractive ($E_{\text{BCS}} < 0$), whereas the linear response in the local interaction model is paramagnetic, corresponding to a repulsive effective interaction ($c > 0$).

II. MAGNETIC RESPONSE DUE TO FORWARD SCATTERING

An interesting observation made by the authors of Ref.¹⁰ is that an effective interaction different from the local interaction used by AE can lead to a much larger persistent current, at least for sufficiently small flux, where it is allowed to calculate the current from the linear response. Given the rather crude approximations in the microscopic derivation of the local interaction model, it seems worthwhile to explore the magnetic response for other types of effective interactions. A possibility which so far has not been thoroughly analyzed is an interaction which is dominated by small momentum transfers. Note that the assumption that only forward scattering processes (corresponding to vanishing momentum transfer) have to be taken into account for a consistent description of the low-energy and long-wavelength properties of normal metals lies at the heart of the Landau's Fermi liquid theory. The Landau model is in a sense the opposite extreme of the local interaction model, because the effective interaction in the Landau model is proportional to a Kronecker-delta in momentum space,

$$\overline{V}_e(\mathbf{q}; i!) = \epsilon_0 f_0 \delta_{\mathbf{q}, 0}; \quad (10)$$

where the Landau parameter f_0 can be determined from experiments. In fact, the dimensionless Landau parameter¹¹ $F_0 = 2 \epsilon_0 f_0$ can be written as $F_0 = \frac{B m}{B_0 m_0} \ll 1$, where B is the bulk modulus, m is the effective mass, and B_0 and m_0 are the corresponding quantities in the absence of interactions. Inserting the known bulk values

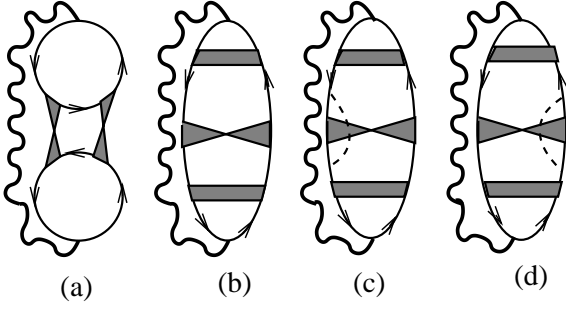


FIG. 3: Feynman diagrams that dominate the flux-dependent part of the grand canonical potential if the effective interaction involves only momentum transfers smaller than the inverse elastic mean free path, $1/\ell$. For vanishing momentum transfer the Hartree diagram (a) dominates the linear magnetic response, whereas outside the regime of validity of linear response the sum of the three Fock diagrams (b)-(d) has the same order of magnitude as the Hartree diagram (a). Note that the Dyson (shaded box, see Fig. 2) renormalizes only the density vertex in the Fock diagrams; the interaction in the Hartree diagram does not transfer any energy and hence cannot be renormalized by singular Dyson corrections.

for Cu^{12} , $m = 1.3$ and $B = B_0 = 2.1$, we find $F_0 = 1.7$, which is a factor of 30 larger than the corresponding estimate $c = 0.06$ in the local interaction model. Note that in real space Eq. (10) corresponds to a constant effective interaction, proportional to the inverse volume of the system

$$\bar{V}_e(\mathbf{r} = \mathbf{r}') = \frac{f_0}{V} : \quad (11)$$

Given an effective interaction of the form (10), the dominant flux-dependent contributions to the average potential $\bar{\epsilon}(\mathbf{r})$ to first order in the interaction are shown in Fig. 3. The Fock diagrams (b)-(d) have been discussed previously in Refs.^{13,14}; as first pointed out by Beal-Monod and Montambaux¹³, to leading order in the small parameter $(k_F \ell)^{-1}$, the three Fock diagrams in Fig. 3 (b)-(d) cancel, so that a direct evaluation of the sum of these diagrams is rather difficult. To calculate the leading contribution of these diagrams, we note that the fermion loops in Fig. 3 (b)-(d) can be identified with contributions to the disorder averaged polarization, which for general frequencies and small wavevectors can be written as¹⁵

$$\bar{\Pi}_0(\mathbf{q}; i!) = 2 \int_0^{\infty} \frac{D(i!) q^2}{D(i!) q^2 + j! j} ; \quad (12)$$

where $D(i!)$ is a generalized frequency-dependent Dyson coefficient. The crucial observation is now that the sum of the three Fock diagrams in Fig. 3 (b)-(d) corresponds to the usual weak localization correction to the average conductance¹⁴,

$$D(i!) = D_0 [1 + g_{WL}(i!)] ; \quad (13)$$

where

$$g_{WL}(i!) = \frac{2}{\pi} \int_0^{\infty} \frac{1}{D_0 q^2 + j! j} : \quad (14)$$

Essentially we have used the equation of continuity to replace the charge vertices in Fig. 3 by current vertices, which cannot be renormalized by singular diffusion corrections. The fact that a gauge transformation replacing charge vertices by current vertices can be used to avoid the explicit calculation of vertex corrections has also been employed in Ref.¹⁶ to calculate the zero bias anomaly in the tunneling density of states of two-dimensional disordered electrons interacting with Coulomb forces.

The evaluation of the contribution of the three Fock diagrams in Fig. 3 to the persistent current is now straightforward. Note that for a thin ring with $L \ll \ell$ the q -summation is one-dimensional, with quantized wavevectors $2(n + 1/2)/L$, $n = 0; 1; 2; \dots$. Then we obtain for the k -th Fourier component of the average current due to the Fock diagrams (b)-(d) in Fig. 3 for the Landau model¹⁴,

$$I_k^{L, \text{Fock}} / k = \frac{f_0}{V} : \quad (15)$$

Due to the extra factor of inverse volume, this contribution is, for experimentally relevant parameters¹, negligible compared with corresponding result in the local interaction model given in Eq. (6).

The Hartree diagram in the Landau model is more interesting. The fact that the diagram with two Cooperons shown in Fig. 3 (a) dominates the persistent current due to electron-electron interactions with momentum transfers $1/\ell$ has already been pointed out in Ref.¹⁷. A similar diagram with two Cooperons (but without interaction line) dominates the fluctuations of the number of energy levels in a fixed energy window centered at the Fermi energy¹⁸. Using the approximate relation

$$I_N(\epsilon) = \frac{c}{2} \frac{\partial \langle N^2 \rangle}{\partial \epsilon} \quad (16)$$

between the persistent current $I_N(\epsilon)$ at constant particle number and the fluctuation $\langle N^2 \rangle$ of the particle number at constant chemical potential ϵ , several authors have realized^{19,20,21} that without interactions the two-Cooperon diagram determines the average persistent current in a canonical ensemble. Note that the Hartree diagram in Fig. 3 (a) does not contain any vertex corrections analogous to the diffusion corrections of the vertices in the Fock diagrams (b)-(d). This is due to the fact that the interaction line in the Hartree process does not transfer any energy. Hence, the two Green functions attached to the vertex of a Hartree interaction are either both retarded or both advanced, so that it is impossible to attach a singular Dyson to the vertex.

For the Landau model the Hartree diagram in Fig. 3 (a) yields at finite temperature T the following correction

clarify this point, a better microscopic theory of the effective electron-electron interaction in mesoscopic disordered metals is necessary. In particular, a microscopic theory should properly treat the problem of screening in a finite system and incorporate the breakdown of Fermi

liquid theory in quasi-one-dimensional disordered metals at sufficiently low temperatures²⁴.

We thank M. Schechter for his clarifying remarks concerning Ref.¹⁰ and for his comments on this manuscript.

-
- ¹ L. P. Levy, G. Dolan, J. Dunsmuir, and H. Bouchiat, Phys. Rev. Lett. 64, 2074 (1990).
- ² Y. Imry, Introduction to Mesoscopic Physics (Oxford University Press, Oxford, 1997).
- ³ U. Eckern and P. Schwab, J. Low Temp. Phys. 126, 1291 (2002).
- ⁴ P. Mohanty, Ann. Physik (Leipzig) 8, 549 (1999).
- ⁵ E. M. Q. Jariwala, P. Mohanty, M. B. Ketchen, and R. A. Webb, Phys. Rev. Lett. 86, 1594 (2001).
- ⁶ V. Ambegaokar and U. Eckern, Phys. Rev. Lett. 65, 381 (1990).
- ⁷ We prefer to express the response in terms of the normal flux quantum $\phi_0 = hc/4e$, whereas $\phi_0 = hc/2e$ in Ref.¹⁰ is the superconducting flux quantum. This is the reason why the numerical prefactor in our Eq. (8) is 32, while the corresponding prefactor in Eq. (1) of Ref.¹⁰ is 8.
- ⁸ A. Volker and P. Kopietz, Mod. Phys. Lett. B 10, 1397 (1996).
- ⁹ U. Eckern, Z. Phys. B 82, 393 (1991).
- ¹⁰ M. Schechter, Y. Oreg, Y. Imry, and Y. Levinson, Phys. Rev. Lett. 90, 026805 (2003).
- ¹¹ Note that we define ρ_0 to be the density of states per spin, so that $F_0 = 2\rho_0 f_0$ agrees with the usual definition of the dimensionless Landau parameter.
- ¹² N. W. Ashcroft and N. D. Mermin, Solid State Physics, (Holt-Saunders, Philadelphia, 1976).
- ¹³ M. T. Beal-Monod and G. Montambaux, Phys. Rev. B 46, 7182 (1992).
- ¹⁴ P. Kopietz and A. Volker, Phys. Lett. A 244, 569 (1998).
- ¹⁵ D. Vollhardt and P. Wolfe, Phys. Rev. B 22, 4666 (1980).
- ¹⁶ P. Kopietz, Phys. Rev. Lett. 81, 2120 (1998).
- ¹⁷ P. Kopietz, Phys. Rev. Lett. 70, 3123 (1993); erratum: 71, 306 (1993).
- ¹⁸ B. L. Altshuler and B. I. Shklovskii, Zh. Eksp. Teor. Fiz. 91, 220 (1986) [Sov. Phys. JETP 64, 127 (1986)].
- ¹⁹ A. Schmid, Phys. Rev. Lett. 66, 80 (1991).
- ²⁰ F. von Oppen and E. K. Riedel, Phys. Rev. Lett. 66, 84 (1991).
- ²¹ B. L. Altshuler, Y. Gefen, and Y. Imry, Phys. Rev. Lett. 66, 88 (1991).
- ²² I. J. Pomerenchuk, Zh. Eksp. Teor. Fiz. 35, 524 (1958) [Sov. Phys. JETP 8, 361 (1958)].
- ²³ G. Murthy and R. Shankar, Phys. Rev. Lett. 90, 066801 (2003); D. Hermann, H. Mathur, and G. Murthy, Phys. Rev. B 69, 041301 (2004); G. Murthy, R. Shankar, D. Hermann, and H. Mathur, ibid. 69, 075321 (2004).
- ²⁴ B. L. Altshuler and A. G. Aronov, in Electron-Electron Interactions in Disordered Systems, edited by A. L. Efros and M. Pollak, (North Holland, Amsterdam, 1985).